ELSEVIER

Biochimica et Biophysica Acta 1233 (1995) 75–83

BBA Biochimica et Biophysica Acta

Sterols stabilize the ripple phase structure in dihexadecylphosphatidylcholine

B.A. Cunningham [a,*], L. Midmore [a], O. Kucuk [b,1], L.J. Lis [b], M.P. Westerman [b], W. Bras [c], D.H. Wolfe [d], P.J. Quinn [e], S.B. Qadri [f]

[a] *Department of Physics, Bucknell University, Lewisburg, PA 17837, USA*
[b] *Division of Hematology / Oncology, UHS / The Chicago Medical School, The Veterans Affairs Medical Center, N. Chicago, IL 60064 and Mount Sinai Medical Center, Chicago, IL 60608, USA*
[c] *Netherlands Organization for Scientific Research (NWO) / Science and Engineering Research Council, Daresbury Laboratory, Warrington WA4 4AD, UK*
[d] *Department of Astronomy and Physics, Lycoming College, Williamsport, PA 17701, USA*
[e] *Department of Biochemistry, King's College, London, Campden Hill Road, London W8 7AH, UK*
[f] *Naval Research Laboratory, Washington, DC 20375, USA*

Received 31 May 1994; accepted 30 September 1994

Abstract

The presence of various sterols in mixtures with dihexadecylphosphatidylcholine (DHPC) was studied using static X-ray diffraction of temperature equilibrated samples, and real-time X-ray diffraction of samples undergoing temperature scans. It was found that these sterols eliminate the interdigitation of the alkyl chains in the DHPC sub-gel and gel-state bilayers while stabilizing the ripple gel-state at the expense of the gel-state bilayer phase. The ripple–ripple phase transition previously observed for dipalmitoylphosphatidylcholine in the presence of low molar concentrations of sterols (Wolfe et al. (1992) Phys. Rev. Lett. 68, 1085–1088) was also observed for similar DHPC-sterol mixtures. In addition, we show the first evidence that the presence of 5α-cholestane-3β,5,6β-triol will cause the lipid mixtures to continue to adopt a ripple mesophase structure even after the DHPC alkyl chain becomes disordered.

Keywords: Sterol; Phospholipid; Ripple phase; X-diffraction; Lipid phase behavior

1. Introduction

Biological membranes consist of a mixture of lipids and proteins that provide a structural backbone and mediate the mechanism(s) for various biological functions. Plasma membranes are relatively unique in having cholesterol as one of their major components. A large effort over many years has provided us with a general knowledge of how cholesterol can be incorporated into a lipid membrane [1,2]. X-ray diffraction studies have been useful in the interpretation of calorimetric and spectroscopic observations by defining the lipid phases created by the presence of varying amounts of cholesterol [3–5]. Recent technological changes in X-ray sources have provided the most definitive structural assignments [6,7].

The phase structures and transitions of dihexadecylphosphatidylcholine (DHPC) have been examined by several researchers. Laggner et al. [8], Ruocco et al. [9], and Kim et al. [10] have previously shown that this lipid at full hydration can form interdigitated crystalline and gel-state bilayers, ripple phases, and disordered state bilayers with increasing temperature (see Fig. 1). It has been reported that 'high' concentrations of cholesterol (20 mol% [11] and 50 mol% [12]) eliminate the hydrocarbon chain interdigitation in the gel phase of DHPC. More recently, Laggner et al. [13] have reported that cholesterol contents as low as 0. 1 mol% and as high as 5 mol% perturb DHPC interdigitation leading to the presence of coexisting interdigitated and non-interdigitated lamellar gel phases. This conclusion is based on the presence of X-ray diffraction peaks that could be resolved into patterns from bilayers

* Corresponding author. Fax: +1 (717) 5243760.
[1] Present address: Cancer Research Center of Hawaii, 1236 Lauhala Street, Honolulu, HI 96813, USA.

SSDI 0005-2736(94)00240-1

with a small *d*-spacing and others with a significantly increased *d*-spacing. This observation is similar to a previous diffraction report [4] and spectroscopic and calorimetry report [14] which, at that time, interpreted from their results the presence of two coexisting gel-state bilayers for dipalmitoylphosphatidylcholine (DPPC) in the presence of less than 10 mol% cholesterol. Recent high resolution X-ray data [5] has shown that the correct interpretation is that of a cholesterol stabilized DPPC gel-state ripple bilayer phase ($P_{\beta'}$).

In this report, we examined a DHPC plus 5 mol% cholesterol mixture using high resolution and real-time X-ray diffraction to determine if a ripple bilayer was present. In addition, similar mixtures of DHPC with the oxidized sterols 7-ketocholesterol and 5α-cholestane-3β,5,6β-triol were examined to determine what effect a change in interfacial DHPC-sterol interactions had on the stability of the ripple bilayer phase.

We have confirmed from dynamically collected X-ray diffraction patterns and high resolution static X-ray diffraction patterns the phase sequence for fully hydrated DHPC to be a lamellar phase with interdigitated hydrocarbon chains in orthorhombic packing ($L_{i,o}$), a lamellar phase with interdigitated chains in hexagonal packing ($L_{i,h}$), ripple phase bilayers ($P_{\beta'}$), and disordered bilayer phase (L_α) as a function of increasing temperature. The presence of 5 mol% of various sterols (cholesterol, 7-ketocholesterol, or 5α-cholestane-3β,5,6β-triol) was observed to cause the elimination of the DHPC interdigitated 'gel-state' bilayer ($L_{i,h}$) resulting in a direct transition between a non-interdigitated 'crystalline' (L_c) phase and the $P_{\beta'}$ phase. In addition, the ripple–ripple phase transition previously reported for DPPC-sterol mixtures was also observed for the DHPC-sterol mixtures examined. Theoretical work by a number of researchers [15–21] have provided a framework for explaining the molecular cause of both ripple and interdigitated bilayer phase formation and stabilization. In addition, we report for the first time a ripple phase in a disordered alkyl chain state lipid phase for mixtures of DHPC and 5 mol% 5α-cholestane-3β,5,6β-triol.

2. Materials and Methods

2.1. Materials

DHPC was obtained from Sigma (St. Louis, MO) and used without further purification. Cholesterol was obtained from Sigma (St. Louis, MO), and 7-ketocholesterol and 5α-cholestane-3β,5,6β-triol from Steraloids (Wilton, NH). Water was distilled and all other solvents and chemicals were reagent grade.

2.2. Sample preparation

Known weights of DHPC and sterol were co-mixed in chloroform. The chloroform was subsequently evaporated under a stream of N_2 gas with final drying done under high vacuum. Although the solvent could impart an inhomogeneous deposition of the lipid species in the mixing process, our data supports the presence of uniformly mixed

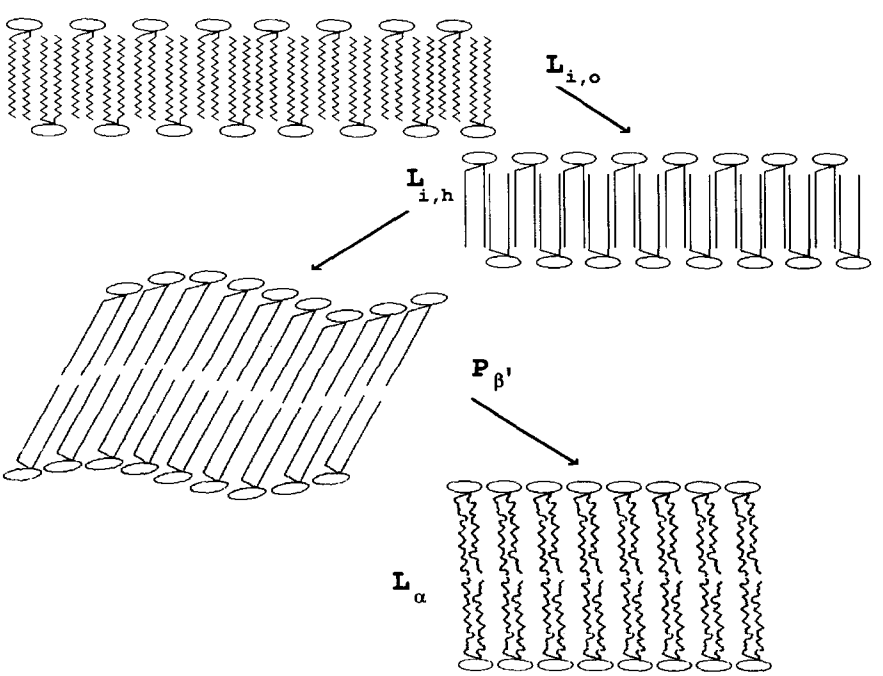

Fig. 1. Phase structures for fully hydrated DHPC. $L_{i,o}$ and $L_{i,h}$ are lamellar phases with interdigitated hydrocarbon chains in orthorhombic and hexagonal packing, respectively; $P_{\beta'}$, is the 'rippled' lamellar phase; and L_α is the disordered lamellar phase.

molecular species without any residual solvent remaining, since we do not observe indications of multiple mesophase or hydrocarbon chain structures in 'single phase' subgel, gel, or disordered hydrocarbon chain phase regions. This observation is consistent with previous studies of similar lipid systems [22–26]. Lipids were then hydrated by heating to approximately 60°C and/or freeze–thaw cycles in the presence of 66.7 wt.% distilled water until no powder was detected. The samples were subsequently stored at approx. O°C or −20°C for 1–3 days before examination. Samples were transported to the beamlines on ice and transferred to a pre-cooled temperature block. Samples for real-time examination were lowered to −50°C before the initial heating cycle was started.

2.3. Static X-ray diffraction

The static X-ray diffraction data were collected at beamline X23B at the National Synchrotron Light Source (NSLS) at Brookhaven National Laboratory. This beamline, operated by Naval Research Laboratory, has a platinum-coated fused silica toroidal mirror to focus the X-ray beam. In addition, a double flat crystal monochromator was used to select 8.00 keV X-rays from the radiation continuum. The incident X-rays were focused to a spot size of 2 mm × 2 mm. Samples were mounted in aluminum X-ray sample holders along a 3 mm slit in a 1 mm thick Teflon spacer separating two mica windows. The sample holder was placed in an aluminum block and the temperature was controlled by a circulating water bath connected to the sample mount. The temperature was monitored internally using a thermocouple placed adjacent to the sample region of the X-ray sample holder. Diffraction patterns were collected using film or imaging plates (Fuji). Sample-to-film distance was approx. 92 cm to monitor the small-angle X-ray scattering region (for detecting d-spacings down to 20.0 nm) or approximately 10 cm to monitor the wide-angle X-ray scattering region. Spatial calibration was obtained using Teflon [27] and cholesterol [28].

2.4. Real-Time X-ray Diffraction

Real-time X-ray diffraction studies were performed using a monochromatic (0.15 nm) focussed X-ray beam at Station 8.2 of the Daresbury Synchrotron Laboratory. A purpose-built camera allowed clear resolution of reflections between 0.35 nm and 10 nm. The sample holder was a cryostage (Linkam, Tadworth, UK) to which mica windows were fitted. A flow of nitrogen gas at −150°C was passed internally through the sample holder. A TMS90 control system fitted with a remote control unit (Linkam) provided the appropriate amount of power to the heating block of the sample holder to maintain the sample at the desired temperature. Two thermocouples placed adjacent to the sample in the sample holder were used to internally

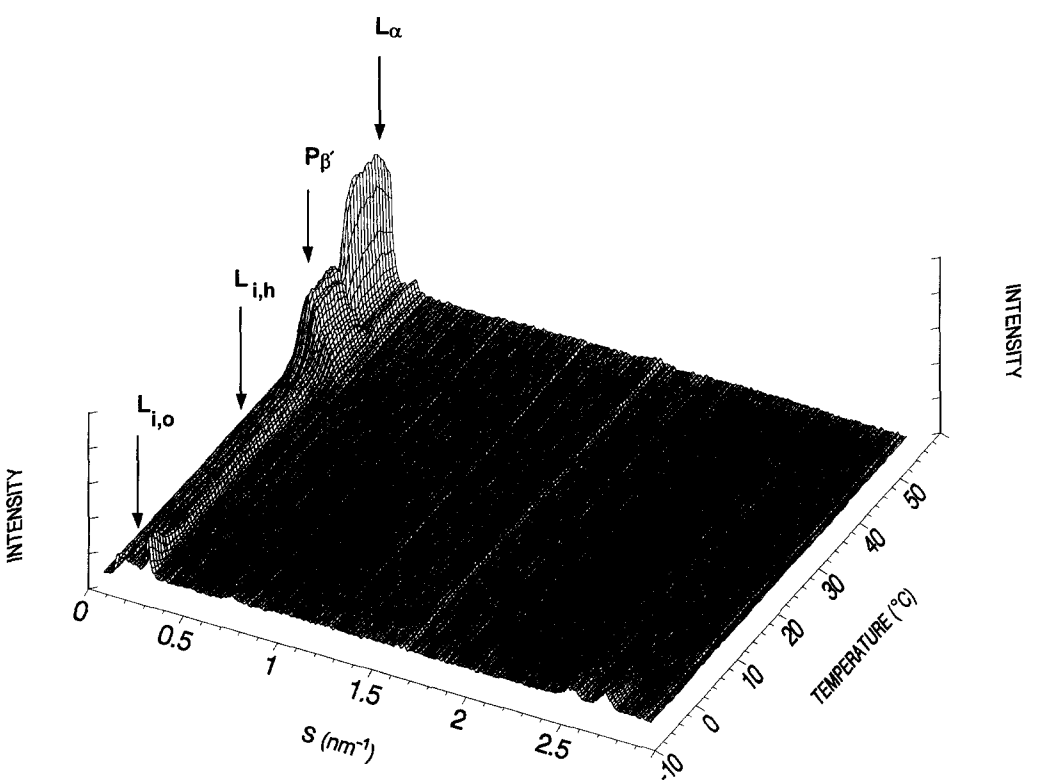

Fig. 2. Three-dimensional plot of X-ray scattering intensity versus reciprocal space (S) as a function of continuously increasing temperature (5°C/min) for fully hydrated DHPC. Every third diffraction pattern of 3 s duration from a total set of 255 continuously recorded patterns are shown.

monitor the temperature. Temperature programming over the range −100°C to 100°C at rates between 0.001°C/min to 2.3°C/s were possible. X-ray data were collected using either a single wire detector or multiwire quadrant detector fabricated at the Daresbury Laboratory. X-ray scattering data was acquired in 255 consecutive time frames separated by a dead time between frames of 50 μs. Data was stored in a VAX 11/785 computer and analyzed using the OTOKO program developed at the Daresbury Laboratory. The detector response was determined by recording the signal from a fixed source accumulated for at least one hour and subtracted from the data. Spatial calibration was obtained using Teflon [27] and cholesterol [28]. Phase transition temperatures were taken as the temperature at which the recorded diffraction peaks started to shift in *d*-spacing or additional peaks from the subsequent phase appeared.

3. Results

Fully hydrated samples of DHPC and DHPC plus 5 mol% cholesterol, 7-ketocholesterol, or 5α-cholestane-3β,5,6β-triol were examined using real-time and high-resolution X-ray diffraction. A typical three-dimensional plot of scattering intensity versus reciprocal spacing ($S = 1/d$) as a function of temperature for fully hydrated DHPC undergoing a temperature scan of 5°C/min is shown in Fig. 2. Representative small and wide angle (SAXS and WAXS) diffraction patterns from Fig. 2 for the four DHPC phases are shown in Fig. 3. Peak assignments are also indicated on the Fig. 3. A summary of *d*-spacing as a function of temperature for fully hydrated DHPC is shown in Fig. 4a with the appropriate phase transitions indicated. Structural parameters and transition temperatures determined from real-time X-ray diffraction data are listed in Table 1. Laggner et al. [8], Ruocco et al. [9], and Kim et al. [10] have previously characterized the fully hydrated DHPC system using temperature equilibrated samples and have shown that heating of the sample yields the phase sequence: $L_{i,o} \rightarrow L_{i,h} \rightarrow P_{\beta'} \rightarrow L_{\alpha}$.

Our data is consistent with the structural parameters for all four phases and transition temperatures for the three phase changes determined previously for this system [8–10]. We can independently infer that the induced DHPC $L_{i,o}$ and $L_{i,h}$ bilayer phases have interdigitated hydrocarbon chains by comparison with the previously reported repeat spacings for the DHPC interdigitated gel-state bilayer [8] and DPPC, an analogue of DHPC, non-interdigitated subgel and gel state bilayers [29]. The relatively small *d*-spacings for the DHPC $L_{i,o}$ and $L_{i,h}$ phases are an indication that the chains are probably fully interdigitated. The assignment of the $P_{\beta'}$ phase is consistent with previous assignments for the diffraction peaks produced by the two-dimensional ripple phase rectangular unit cell in phospholipid systems [5,28]. The presence of ordered or disordered alkyl chains was deduced from observations of the high-angle diffraction peaks produced by hydrocarbon chain packing structures [30,31]. The data presented in Figs. 2 and 4a can thus be interpreted to indicate the following thermally induced dynamic phase transition sequence for fully hydrated DHPC: $L_{i,o} \rightarrow L_{i,h} \rightarrow P_{\beta'} \rightarrow L_{\alpha}$.

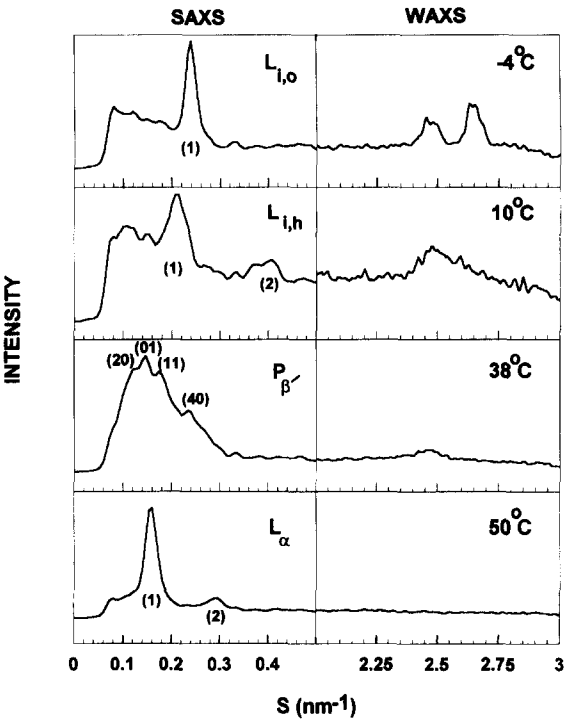

Fig. 3. Representative small- and wide-angle (SAXS and WAXS) diffraction profiles for the $L_{i,o}$, $L_{i,h}$, $P_{\beta'}$, and L_{α} phases observed for fully hydrated DHPC multilayers. Numbers in parentheses correspond to the integer orders ($n = 1$–3) of a one-dimensional lamellar lattice or to the *h*,*k*-indices of a rectangular lattice where the ripple phase is present. These single frames are from the data set presented in Fig. 2 in which the sample was heated at a rate of 5°C/min.

Figs. 4b–d shows *d*-spacings as a function of temperature for typical real-time diffraction data collected for mixtures of DHPC plus 5 mol% cholesterol, 5α-cholestane-3β,5,6β-triol, or 7-ketocholesterol undergoing heating scans of 5°C/min. Structural data and transition temperatures derived from real-time X-ray diffraction data for DHPC plus 5 mol% cholesterol, 7-ketocholesterol, or 5α-cholestane-3β,5,6β-triol are listed in Table 1. The transition temperatures for DHPC plus 5 mol% cholesterol are consistent with the onset temperatures for calorimetric peaks shown by Laggner et al. [13] for the same system. In all the DHPC and sterol samples, the presence of multiple alkyl chain diffraction peaks are observed from the diffraction pattern of the initial phase structure. This is indicative of the presence of crystalline alkyl chain packing. An increase in the *d*-spacing for DHPC and sterol mixtures relative to pure DHPC indicates that the lamellar crystalline phase contains only non-interdigitated phases. In all cases, the L_c phase for these mixtures transforms under continuous heating directly into a ripple phase. This phase

is characterized (as for pure DHPC) by its complex diffraction patterns consisting of apparently overlapping patterns from a number of lamellar repeat units [5,8,28]. The peak assignments have been previously reported for pure phospholipid ripple phases and are assumed to be the same for these lipid systems [5,28]. We rule out a phase separation of lamellar phases in this region because of the presence of a single phase region on cooling the sample into the L_c structure. We observe a ripple–ripple phase transition for all the DHPC-sterol mixtures. A ripple–ripple transition has been previously reported for similar DPPC-sterol mixtures [5]. All lipid mixtures except DHPC plus 5 mol% 5α-cholestane-3β,5,6β-triol produced the expected disordered lipid bilayer (L_α) phase upon thermally induced transformation from the $P_{\beta 2'}$, phase. However, the $P_{\beta 2'}$ phase for DHPC plus 5 mol% 5α-cholestane-3β,5,6β-triol transformed upon heating into a ripple phase with disordered alkyl chains (P_α) as evidenced by the change in the wide-angle alkyl chain diffraction. The P_α mesophase is characterized by its complex small angle X-ray scattering pattern. Fig. 5 shows representative X-ray diffraction patterns of the $P_{\beta 1'}$ and P_α phases for DHPC in the presence of 5 mol% 5α-cholestane-3β,5,6β-triol. Assignments for the two-dimensional diffraction peaks are listed on Fig. 6 and consistent with a rectangular ripple phase unit cell. Thus the presence of cholesterol or 7-ketocholesterol is sufficient to change the DHPC thermally induced dynamic phase transition sequence from $L_{i,o} \rightarrow L_{i,h} \rightarrow P_{\beta'} \rightarrow L_\alpha$ to $L_c \rightarrow P_{\beta 1'} \rightarrow P_{\beta 2'} \rightarrow L_\alpha$, while the presence of 5α-cholestane-3β,5,6β-triol induced the sequence $L_c \rightarrow P_{\beta 1'} \rightarrow P_{\beta 2'} \rightarrow P_\alpha$.

Similar samples were also examined using static X-ray diffraction by equilibration at specific temperatures. In all cases, the phases and *d*-spacings obtained were consistent with those obtained in real-time experiments while the sample was undergoing a temperature scan. All ripple wavelengths were determined from static X-ray diffraction measurements. From the data in Table 1, it appears that the greater the oxidation, the smaller the ripple wavelength. Furthermore, the ripple wavelength for DHPC plus 5 mol% 5α-cholestane-3β,5,6β-triol decreases from $\approx$ 19 nm to $\approx$ 18 nm when the P_α phase is kept at a temperature of approximately 60°C for about two hours (data not shown). We also observed a decrease in the mesophase *d*-spacing from 7.2 nm to 6.4 nm for DHPC plus 5 mol% 5α-cholestane-3β,5,6β-triol in the P_α phase under these same conditions.

The above results infer a role for small cholesterol

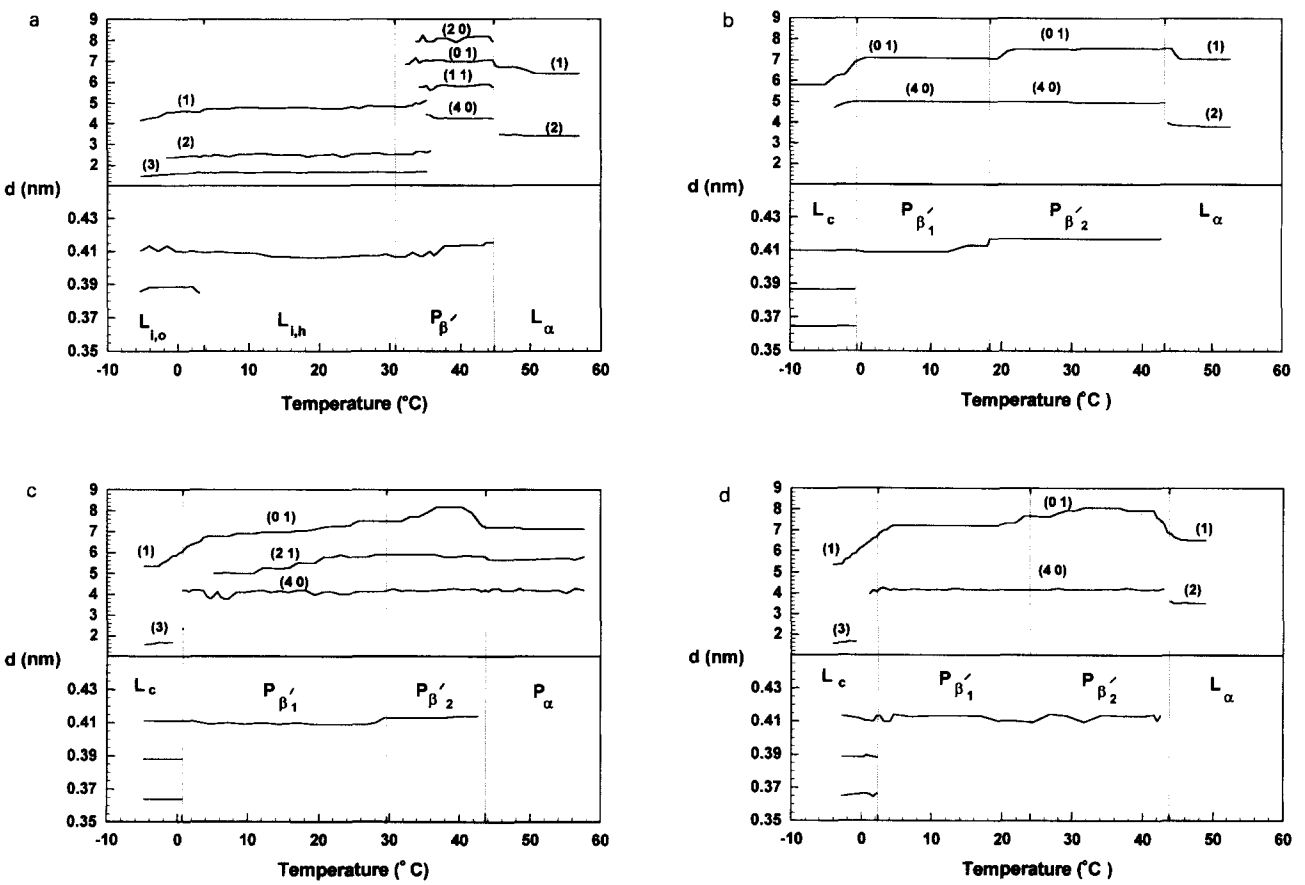

Fig. 4. Repeat spacings of the small-angle and wide-angle X-ray scattering regions as a function of temperature for fully hydrated (a) DHPC, (b) DHPC plus 5 mol% cholesterol, (c) DHPC plus 5 mol% 5α-cholestane-3β,5,6β-triol, and (d) DHPC plus 5 mol% 7-ketocholesterol. Numbers in parentheses correspond to the integer orders ($n = 1$–3) of a one-dimensional lamellar lattice or to the *h*,*k*-indices of a rectangular lattice where the ripple phase is present. Vertical lines indicate approximately the phase boundaries.

concentrations in stabilizing the gel-state ripple bilayer phase in DHPC. This is consistent with our previous observations of a similar sterol effect on DPPC dispersions. Unfortunately, high luminosity X-ray sources must be used to unequivocally assign the presence of a ripple phase on the basis of X-ray diffraction data. We [4] and others [13] have erroneously assigned a two phase bilayer region to this portion of the cholesterol–phospholipid phase diagram based on lower resolution X-ray diffraction data. In addition, the calorimetrically recorded pre-transition peaks for DHPC plus low cholesterol content mixtures can now be correctly assigned to a transition between gel-state ripple bilayer phases with differing water separations as previously reported for similar DPPC-cholesterol mixtures [5].

4. Discussion

The most surprising result of this study is the presence of ripples in the disordered state of the mixture of DHPC and 5α-cholestane-3β,5,6β-triol. This phase has not previously been observed in phospholipid-sterol model membranes. However, a $P_{\alpha\beta}$ (or P_γ) phase, a ripple phase with both disordered and gel state acyl chains, was initially observed by Luzzati et al. [32], and was shown to occur in low temperature, dehydrated egg lecithin [30] and in low hydrated dipalmitoylphosphatidylcholine bilayers [33]. This phase has been proposed to consist of disordered acyl chains in the curved portion of the sinusoidal ripple phase and gel-state acyl chains in the bilayer portion of the ripple. It was further proposed that for greater gel-state lipid contents and, therefore, larger regions of bilayers in the ripple (long ripple wavelengths), the gel-state acyl chain diffraction peaks would increase and become recordable. In none of the samples of DHPC plus 5 mol% 5α-cholestane-3β,5,6β-triol studied was there evidence of gel-state alkyl chain diffraction peaks in the P_α phase. This is consistent with our own observations of a relatively small ripple wavelength with this system. We can rule out that heating above 60°C or equilibrating for extended periods of time above T_m would eventually lead to a transition to the L_α phase since static X-ray diffraction for a sample equilibrated at 65°C for approximately two hours showed no phase transition.

Laggner et al. [13] have proposed that line boundaries

Table 1
Structural parameters and transition temperatures for phases produced by fully hydrated DHPC admixtures containing 5 mol% sterols

Sterol	Phase	Mesophase *d*-spacings (nm) [a,b]	Acyl chain scattering peaks (nm)	Transition temperatures (°C) [c]
None	$L_{i,o}$	4.53	0.41, 0.39	
				3.7
	$L_{i,h}$	4.69	0.41	
				32.3
	$P_{\beta'}$	7.00 (≈ 20.0)	0.41	
				45.3
	L_α	6.73	–	
Cholesterol	L_c	≈ 5.8	0.41, 0.39, 0.36	
				0.7
	$P_{\beta 1'}$	7.10 (≈ 21.0)	0.41	
				19.6
	$P_{\beta 2'}$	7.54 (≈ 21.0)	0.42	
				42.8
	L_α	7.04	–	
5α-Cholestane-3β,5,6β-triol	L_c	5.67	0.41, 0.39, 0.36	
				0.2
	$P_{\beta 1'}$	6.76 (≈ 16.0)	0.41	
				32.9
	$P_{\beta 2'}$	8.17 (≈ 16.0)	0.41	
				41.6
	P_α	7.21 (≈ 19.0)	–	
7-Ketocholesterol	L_c	5.36	0.41, 0.39, 0.36	
				0.7
	$P_{\beta 1'}$	7.22 (≈ 16.0)	0.41	
				20.7
	$P_{\beta 2'}$	8.07 (≈ 16.0)	0.41	
				42.1
	L_α	6.66	–	

[a] $L_{i,o}$ or L_c mesophase *d*-spacings were determined at −5°C. All other mesophase *d*-spacings were determined approx. 2°C past the transition temperature.
[b] All ripple dimensions in parentheses were determined from static X-ray diffraction of temperature equilibrated samples.
[c] Phase transition temperatures were determined from heating scans of 5°C/min.

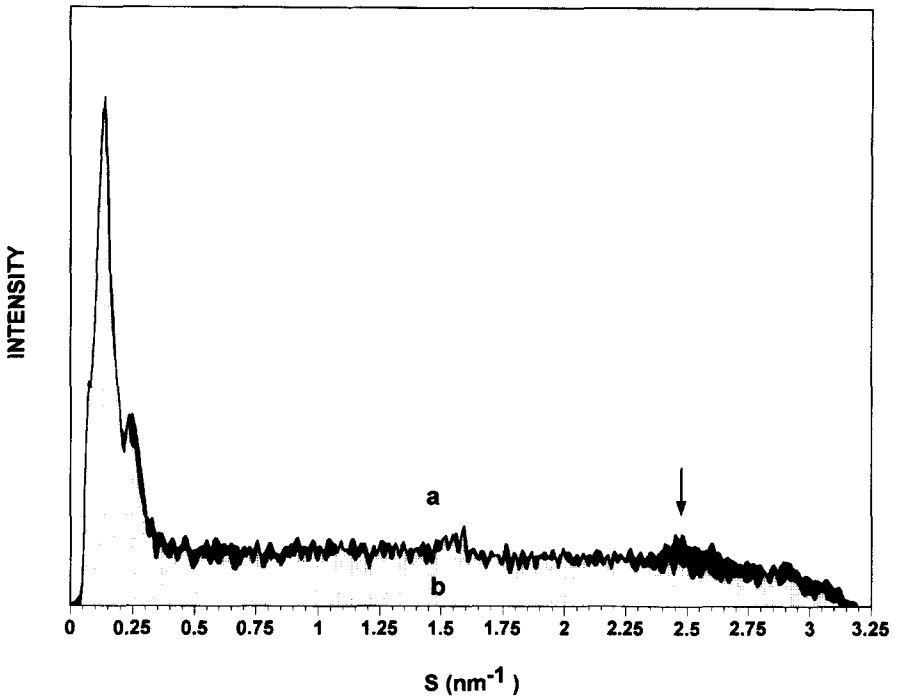

Fig. 5. Diffraction profile of DHPC plus 5 mol% 5α-cholestane-3β,5,6β-triol in (a) the ripple $P_{\beta 1'}$ phase at 11.0°C and (b) the ripple P_{α} phase at 52.0°C. Arrow indicates the presence or absence of the alkyl chain reflection.

between dissimilar phospholipid phase domains are part of the mechanism of cholesterol interactions in membranes. Our data is consistent with this proposal although the phase domains that we refer to consist of lipids with ordered or disordered hydrocarbon chain packing [30]. The mechanical stress produced by the mismatch between the lipid packing in these domains could lead to production of buckling or undulations within a biological membrane. This is consistent with observations of sterol-induced changes in red blood cell morphology involving curvature [34].

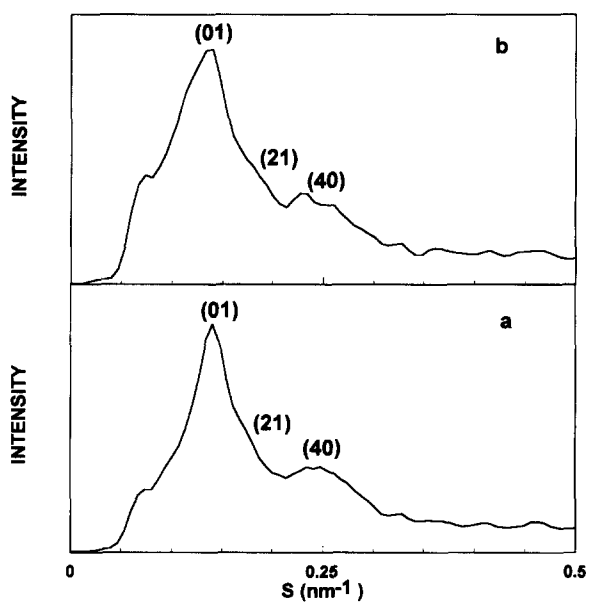

Fig. 6. Comparison of the small angle X-ray diffraction peaks of DHPC plus 5 mol% 5α-cholestane-3β,5,6β-triol in (a) the ripple $P_{\beta 1'}$ phase at 11.0°C and (b) the ripple P_{α} phase at 52.0°C. Numbers in parentheses correspond to the *h,k*-indices of a rectangular lattice.

Although all structural parameters such as water separation and bilayer thickness change with increasing temperature, we can compare *d*-spacing values for the ripple ($P_{\beta'}$) systems by using X-ray patterns obtained just after the completion of the phase transition. During the phase transition itself, absorbed energy is used in promoting the transformation of the initial phase and, therefore, is not used to increase the thermal motion of the individual phases. There is little change in either the L_c or $P_{\beta'}$ phase structural parameters during this transition. A comparison of comparable $P_{\beta'}$ phase bilayer repeat parameters indicates that the presence of sterols decreases the DHPC $P_{\beta'}$ phase bilayer repeat spacings in the order: cholesterol > none > 7-ketocholesterol > 5α-cholestane-3β,5,6β-triol. Thus, the greater the oxidation of the sterol the more it disrupts the interactions between DHPC molecules. We also note that the ripple repeat spacings have roughly the same sequence. We cannot ascertain from this data whether the change in *d*-spacing is due to a change in water layer thickness or bilayer separation, or both, although one can present an hypothesis consistent with Cevc's theory of ripple phase formation [21].

A number of theories have been presented which describe a variety of macroscopic phenomenological approaches and microscopic approaches to predicting ripple phase formation and stability [15–21] in multilamellar

lipid arrays. In order to describe the bulk formation of lipid phases, Goldstein and Leibler [20] used a Landau–Ginsburg Hamiltonian. The ripple phase was characterized by the consideration of spatial variations within the envelope of the membrane thickness. On a macroscopic scale, Cevc [21] has indicated that intramembrane lipid headgroup interactions probably drive the formation of the ripple phase. Cevc has predicted that as headgroup interactions become stronger the lipid dispersions would transform directly from the sub-gel (L_c) into the rippled ($P_{\beta'}$) phase without an intermediate gel state bilayer ($L_{\beta'}$) being formed, and that the wavelength of a ripple would be inversely proportional to the hydration state of the lipid. An extreme case for this theory at high hydrations (and strong chain–chain interactions) is the interdigitated bilayer. The above theories have been generated for phase formation in pure, single-component lipid systems. A headgroup pair-wise potential would be a necessary addition to the theoretical approach when considering the interactions of additive molecules — i.e., sterols — within a phospholipid bilayer phase. Clearly, a rigorous treatment of ripple phase formation and stability would require consideration of both short-range and long-range order interactions in order to mimic the short wavelength or localized mechanical deformations and the long wavelength or bulk mechanical deformations.

An interdigitated phase, whether in a subgel or gel-state bilayer, would be expected to be stabilized via hydrocarbon chain interactions which impart specific orientations for the headgroups within the bilayer. In order to disrupt this phase, the hydrocarbon chain interactions must be weakened. The ripple phase, however, is driven primarily by intralamellar headgroup–water–headgroup interactions [21]. The stability of the $P_{\beta'}$ phase, as evidenced by a reduction in the 'main-transition' temperature; i.e., the transition temperature of the ripple to disordered phase, of all the sterol and DHPC mixtures (see Table 1), is dependent on the strength of the intralamellar interfacial interactions. Thus, we observe that the presence of sterols eliminates DHPC alkyl chain interdigitation and stabilizes the ripple phase. We can hypothesize that sterols disrupt the packing within the hydrocarbon chain region, and change the orientation of the lipid molecules within the bilayer. In addition, we can hypothesize that this reorientation of the lipid molecules allows their headgroups to increase their interactions and become more close packed which is consistent with factors favoring ripple phase formation. These greater interactions can even allow for the stabilization of the ripple phase even when the lipid hydrocarbon chains are in a disordered state. We would expect that these changes would have opposite effects on lipid bilayer thickness and, to a lesser extent, water layer thickness. That is, to be consistent with the observations of a sterol-induced reduction in the DHPC bilayer thickness in the ripple phase, a favored hypothesis would be for the bilayer to decrease in both bilayer thickness and water separation.

5. Conclusion

We can summarize our results as the following: (i) that DHPC bilayers can form both subgel and gel-state interdigitated bilayer phases; (ii) the presence of sterols eliminate the interdigitation of the DHPC alkyl chains, and stabilizes the $P_{\beta'}$ phase, and induces the presence of a ripple to ripple phase transition; (iii) the presence of some sterols stabilizes the ripple structure even after the DHPC alkyl chains have become disordered; and (iv) the sterols can be inferred to both decrease the interaction between DHPC alkyl chains while increasing the intralamellar interfacial interactions in agreement with previous theories.

Acknowledgements

The authors wish to thank the staff at the Daresbury Laboratory for their assistance during the course of these experiments. This work was supported in part by the Mount Sinai Hospital Service Club (M.P.W.), the VA Merit Review Board (O.K., M.P.W.), the Science and Engineering Research Council of the UK (P.J.Q.), and a Professional Development Grant from Lycoming College (DHW). B.A.C. and L.J.L. also gratefully acknowledge the award of Wellcome Research Travel Grants from the Burroughs Wellcome Fund.

References

[1] Hiu, S.W. and He, N.B. (1983) Biochemistry 22, 1159–1164.
[2] Demel, R.A. and De Kruijff, B. (1976) Biochim. Biophys. Acta 457, 109–132.
[3] Ladbrooke, B.D., Williams, R.M. and Chapman, D. (1968) Biochim. Biophys. Acta 150, 333–340.
[4] Rand, R.P., Parsegian, V.A., Henry, J.A.C., Lis, L.J. and McAlister, M. (1980) Can. J. Biochem. 58, 959–968.
[5] Wolfe, D.H., Lis, L.J., Kucuk, O., Westerman, M.P., Cunningham, B.A., Qadri, S.B., Bras, W. and Quinn, P.J. (1992) Phys. Rev. Lett. 68, 1085–1088.
[6] Laggner, P. (1988) Top. Curr. Chem. 145, 173–202.
[7] Lis, L.J. and Quinn, P.J. (1991) J. Appl. Crystallogr. 24, 48–60.
[8] Laggner, P., Lohner, K., Degovics, G., Müller, K. and Schuster, A. (1987) Chem. Phys. Lipids 44, 31–60.
[9] Ruocco, M.J., Siminovitch, D.J. and Griffin, R.G. (1985) Biochemistry 24, 2406–2411.
[10] Kim, J.T., Mattai, J. and Shipley, G.G. (1987) Biochemistry 26, 6592–6598.
[11] Komatsu, H. and Rowe, E.S. (1991) Biochemistry 30, 2463–2470.
[12] Siminovitch, D.J., Ruocco, M.J., Makriyannis, A. and Griffin, R.G. (1987) Biochim. Biophys. Acta 901, 191–200.
[13] Laggner, P., Lohner, K., Koynova, R. and Tenchov, B. (1991) Chem. Phys. Lipids 60, 153–161.
[14] Vist, M.R. and Davis, J.H. (1990) Biochemistry 29, 451–464.
[15] Doniach, S. (1979) J. Chem. Phys. 70, 4587–4596.
[16] Pearce, P.A. and Scott, H.L. (1982) J. Chem. Phys. 77, 951–958.
[17] Marder, M., Frisch, H.L., Langer, J.S. and McConnell, H.M. (1984) Proc. Natl. Acad. Sci. USA 81, 6559–6561.
[18] McCullough, W.S. and Scott H.L. (1990) Phys. Rev. Lett. 65, 931–934.

[19] Scott, H.L. and Pearce, P.A. (1989) Biophys J. 55, 339–345.
[20] Goldstein, R.E. and Leibler, S. (1988) Phys. Rev. Lett. 61, 2213–2216.
[21] Cevc, G. (1991) Biochim. Biophys. Acta 1062, 59–69.
[22] Epand, R.M. and Bottega, R. (1987) Biochemistry 26, 1820–1825
[23] Levin, I.W., Keihau, E. and Hures, W.C. (1985) Biochim. Biophys. Acta 820, 40–47.
[24] Mortensen, K., Pfeiffer, W., Sackmann, E. and Knoll, W. (1988) Biochim. Biophys. Acta 945, 221–245.
[25] Rooney, M., Yachnin, S., Kucuk, O., Lis, L.J. and Kauffman, J.W. (1985) Biochim. Biophys. Acta 820, 33–39.
[26] Siegel, D.P., Bauschback, J., Alford, D., Ellens, H., Lis, L.J., Quinn, P.J., Yeagle, P.L. and Bentz, J. (1989) Biochemistry 28, 3703–3709.
[27] Bunn, C.W. and Howells, E.B. (1954) Nature 174, 549–551.
[28] Wack, D.C. and Webb, W.W. (1989) Phys. Rev. A 40, 2712–2730.
[29] Tenchov, B., Lis, L.J. and Quinn, P.J. (1987) Biochim. Biophys. Acta 897, 143–151.
[30] Ranck, J.L. (1983) Chem. Phys. Lipids 32, 251–270.
[31] Tardieu, A., Luzzati, V. and Reman, F.C. (1973) J. Mol. Biol. 75, 711–733.
[32] Luzzati, V., Gulik-Krzywicki, T. and Tardieu, A. (1968) Nature 218, 1031–1034.
[33] Albon, N. and Doucet, J. (1983) Chem. Phys. Lipids 33, 375–382.
[34] Yachnin, S., Streuli, R.A., Gordon, L.I. and Hsu, R.C. (1979) Curr. Top. Hematol. 2, 245–271.